Hindawi Publishing Corporation
Mathematical Problems in Engineering
Volume 2014, Article ID 806853, 7 pages
http://dx.doi.org/10.1155/2014/806853

Research Article

Joint Estimation of DOA and Polarization with CLD Pair Cylindrical Array Based on Quaternion Model

Guibao Wang,[1] Haihong Tao,[1] Lanmei Wang,[2] and Cao Zeng[1]

[1] *National Laboratory of Radar Signal Processing, Xidian University, Xi'an 710071, China*
[2] *School of Physics and Optoelectronic Engineering, Xidian University, Xi'an 710071, China*

Correspondence should be addressed to Guibao Wang; gbwang2008@gmail.com

Received 30 December 2013; Revised 1 April 2014; Accepted 22 April 2014; Published 15 May 2014

Academic Editor: Gradimir Milovanović

This paper proposes a quaternion-ESPRIT algorithm for closed-form estimation of direction of arrival (DOA) and polarization, using a cylindrical conformal array configuration. First, the array steering vector and the elevation are estimated using a quaternion eigenvalue decomposition of the data covariance matrix. Second, the azimuth is estimated. Finally, the polarization parameters are estimated using the relationships between the dipoles and the loops. These estimates are automatically matched. Simulation results show that the performance of quaternion method is obviously better than that of the long-vector method.

1. Introduction

In the last decades, thanks to advances in sensor technology, electromagnetic vector sensor (EMVS) array was widely used in source localization. The problems of estimating direction of arrival (DOA) and polarization parameters have been discussed in many articles. The first direction-finding algorithms, explicitly exploiting all six electromagnetic components, have been developed separately by Nehorai and Paldi [1, 2] and Li [3]. The cross-product-based DOA estimation algorithm was first adapted to ESPRIT by Wong and Zoltowski [4–7]. A uni-vector-sensor ESPRIT algorithm was proposed in [8]. The aforementioned six-component electromagnetic vector sensors are called complete EMVS. The incomplete EMVS antenna configurations have been extensively studied by numerous researchers, collocated loop and dipole (CLD) oriented along the z-axis of Cartesian coordinate can measure the electric-field and magnetic-field z-component [9, 10], as shown in Figure 1. It is noteworthy that the polarization parameter estimation using a CLD array is independent of the sources DOA and it requires no prior information of azimuth and elevation angles [11]. This independence can not be applied to other antenna configurations, for example two identical dipoles [12–14], two identical loops [11, 15], dipole and/or loop triad(s) [16, 17], and so forth [18, 19]. In the above-mentioned contributions, the output of each EMVS in the array can be represented as complex-valued vectors, and the data received by the EMVS array is combined into a long vector in series, which is called long-vector mode [20]. Consequently, the relevant estimators destroy locally the vector type of the signal because of the organization of the data into a large vector.

More recently, the problem of estimating the DOA and polarization of the EMVS array within the algebraic system theory for quaternion and its extension has been widely researched [20–27]. Quaternion MUSIC technique was proposed based on the quaternion formalism of the two-component vector sensor array in [21]. The three-component vector sensor was expressed as a biquaternion number, then biquaternion-based MUSIC was proposed in [22]. The six-component electromagnetic vector sensor array was represented by a quad-quaternion model in [20]. The quaternion-ESPRIT algorithm for a crossed-dipole uniform linear array (ULA) was firstly proposed in [23]. The advantages of using quaternion for EMVS are that the local-vector nature of an EMVS array is preserved in multiple imaginary parts, and it could result in a more compact representation and a better estimation of signal subspace. Compared with long-vector method, the quaternion and its extension algorithms are

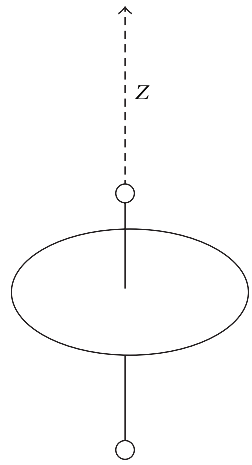

Figure 1: CCCP array element geometry.

shown to be more robust to model errors, while their computation efforts for estimating the data covariance matrices are slightly lower [20–22].

Conformal antenna array, that is, array antennas with antenna elements arranged conformally on a curved surface, is widely used in a variety of airborne radar and other defense systems. The benefits include reduction of aerodynamic drag, wide angle coverage, space savings, and potential increase in available apertures [28–30]. Cylindrical conformal array is a typical conformal array.

The purpose of this paper is to study the quaternion-ESPRIT algorithm for combining DOA and polarization estimation in cylindrical conformal CLD pair (CCCP) array. Compared with loop and dipole pairs oriented along x-axis and y-axis and CDD (cocentered dipole and dipole) pairs, CLL (cocentered loop and loop) pairs oriented along x- and y-axes, respectively, the CLD pairs along the z-axis can decouple the DOA estimation from the polarization estimation [11–15]; errors of DOA and polarization herein do not cumulate. On the contrary, the related algorithms using the other pairs can not decouple the DOA estimation from the polarization estimation, and the DOA and polarization errors in numerical computation accumulate from step to step. The procedure of the proposed method is as follows: first, the array steering vector and the elevation are estimated using a quaternion eigenvalue decomposition of the data covariance matrix. Secondly, the azimuth is estimated using the relationships between direction cosine and spatial steering vector. Thirdly, the polarization parameters are estimated using the relationships between the dipoles and the loops. Hence, this proposed algorithm (1) is computationally less intensive than many open-form search methods; (2) produces closed-form solution with no extra computation needed for signal parameter estimates; (3) resolves the elevation quadrant ambiguity problem; and (4) has the advantage of parameter automatic matching and without spectral peak searching. The simulation results show that the performance of quaternion method is better than that of long-vector method.

2. Definition of Quaternion and Relevant Arithmetic

2.1. Definition of Quaternion. Quaternion, which extended imaginary numbers into a four-dimensional space, began to be developed by William Hamilton in 1843. A complex number has two components: the real and imaginary parts. The quaternion, however, has four components, that is, one real part and three imaginary parts and can be represented in Cartesian form as

$$q = a + ib + jc + kd, \quad a, b, c, d \in R, \tag{1}$$

where a, b, c, and d are real numbers and i, j, and k are complex operators which obey the following rules:

$$\begin{aligned} ij = -ji = k, &\qquad jk = -kj = i, \\ ki = -ik = j, &\qquad i^2 = j^2 = k^2 = -1. \end{aligned} \tag{2}$$

From formulas (1) and (2), quaternion can also be expressed in the following form:

$$q = a + ib + (c + id)\, j = \alpha + \beta j. \tag{3}$$

The quaternion expressed in (3) is also known as the "Cayley-Dickson representation."

2.2. The Relevant Arithmetic of Quaternion. The quaternion conjugate and the quaternion modulus are, respectively, given by

$$q^* = a - ib - jc - kd, \tag{4}$$

$$\|q\| = \sqrt{a^2 + b^2 + c^2 + d^2}. \tag{5}$$

Let q_i be $q_i = a_i + ib_i + jc_i + kd_i$, where a_i, b_i, c_i, and $d_i \in R$, $i = 1, 2$; then the addition of two quaternions expressed in terms of their real and imaginary parts is given by

$$\begin{aligned} q_1 + q_2 = {} & (a_1 + a_2) + i(b_1 + b_2) \\ & + j(c_1 + c_2) + k(d_1 + d_2). \end{aligned} \tag{6}$$

From the rules in (2), it is clear that multiplication is not commutative; namely, $q_1 \cdot q_2 \neq q_2 \cdot q_1$. The inner product of quaternion can be represented as

$$\langle p, q \rangle_H = p^* q. \tag{7}$$

If the inner product of quaternion meets $\langle p, q \rangle_H = 0$, it is said that the quaternions p and q are orthogonal.

From the point of view of algebra, quaternion is an extension of the complex field. A quaternion contains more than two components than that of a complex number, so that it can contain more information in one operation. More details about quaternion can be found in [27].

3. Signal and Array Models

K narrowband completely polarized electromagnetic plane wave source signals impinge upon a CCCP array, which is

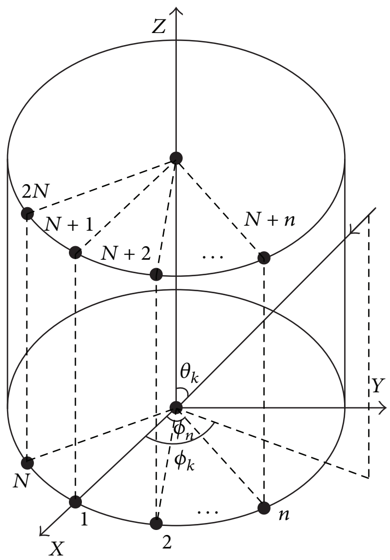

Figure 2: CCCP array geometry.

composed of $2N$ ($N > K$) identical CLD pairs arranged uniformly on the upper and lower circle rings of the cylinder. The distance of the two circle rings is d, which satisfies $d \leq 0.5\lambda_{\min}$, where $\lambda_{\min}$ refers to the minimal signals wavelength of the incident signals. The origin of the Cartesian coordinates is located in the center of the lower circle. Two reference CLD pairs are, respectively, placed at their own center of upper and lower circles. The radii of the upper and lower circles are both R which satisfies $R \leq 0.5\lambda_{\min}$. The first CLD pair located on the cross point of lower circle and the positive x-axis, along the anticlockwise direction is, respectively, the first, second, ..., and Nth CLD pair. Similarly, the $(N+1)$th CLD pair located on the cross point of upper circle and the positive x-axis along the anticlockwise direction is, respectively, the $(N+1)$th and $(2N)$th CLD pair, as shown in Figure 2.

For the CLD pairs, the dipoles parallel to the z-axis are referred to as the z-axis dipoles and the loops parallel to the x-y plane are referred to as the x-y plane loops, respectively, measuring the z-axis electric field components and the z-axis magnetic field components. The CLD pairs' steering vector of the kth ($1 \leq k \leq K$) unit-power electromagnetic source signal is the following 2×1 vector [3]:

$$\mathbf{a} = \begin{bmatrix} e_{kz} \\ h_{kz} \end{bmatrix} = \begin{bmatrix} 0 & -\sin\theta_k \\ \sin\theta_k & 0 \end{bmatrix} \begin{bmatrix} \cos\gamma_k \\ \sin\gamma_k e^{j\eta_k} \end{bmatrix}, \tag{8}$$

where $\theta_k \in [0, \pi]$ is the signals elevation angle measured from the positive z-axis, $\gamma_k \in [0, \pi/2]$ represents the auxiliary polarization angle, and $\eta_k \in [-\pi, \pi]$ symbolizes the polarization phase difference. Both the z-axis electric field e_{kz} and the z-axis magnetic field h_{kz} involve the same factor $\sin\theta_k$, so polarization estimation based on CLD pairs is independent of the sources direction of arrival and it requires no prior information of azimuth and elevation angles.

The e_{kz} and h_{kz} can be expressed as follows with a quaternion c_k:

$$\begin{aligned} c_k &= e_{kz} + i h_{kz} \\ &= -\sin\theta_k \sin\gamma_k e^{j\eta_k} + i \sin\theta_k \cos\gamma_k. \end{aligned} \tag{9}$$

The output of array response for the kth incident signal can be expressed as follows:

$$x_k(t) = \underbrace{c_k \mathbf{q}(\theta_k, \phi_k)}_{\mathbf{a}(\theta_k, \phi_k, \gamma_k, \eta_k)} s_k(t), \tag{10}$$

where $\phi_k \in [0, 2\pi]$ is the azimuth of the kth incident signal and $s_k(t)$ is the kth incident signal. $\mathbf{q}(\theta_k, \phi_k)$ is the spatial steering vector constituted by the phase differences between the array elements and the origin; that is,

$$\mathbf{q}(\theta_k, \phi_k) = \begin{bmatrix} 1 & \mathbf{q}_L^T(\theta_k, \phi_k) & e^{j(2\pi d \cos\theta_k/\lambda)} & \mathbf{q}_U^T(\theta_k, \phi_k) \end{bmatrix}^T, \tag{11}$$

with

$$\mathbf{q}_L(\theta_k, \phi_k) = \begin{bmatrix} e^{j(2\pi R \sin\theta_k \cos(\phi_k - \varphi_1)/\lambda)} & \cdots & e^{j(2\pi R \sin\theta_k \cos(\phi_k - \varphi_N)/\lambda)} \end{bmatrix}^T \tag{12}$$

$$\mathbf{q}_U(\theta_k, \phi_k) = \begin{bmatrix} e^{j(2\pi(R \sin\theta_k \cos(\phi_k - \varphi_1) + d\cos\theta_k)/\lambda)} & \cdots & e^{j(2\pi(R \sin\theta_k \cos(\phi_k - \varphi_N) + d\cos\theta_k)/\lambda)} \end{bmatrix}^T. \tag{13}$$

From (12), the phase of $\mathbf{q}_L(\theta_k, \phi_k)$ can be expressed as

$$\arg\left[\mathbf{q}_L(\theta_k, \phi_k)\right] = \frac{2\pi R}{\lambda} \begin{bmatrix} \beta_k \\ \alpha_k \sin\Delta + \beta_k \cos\Delta \\ \vdots \\ \alpha_k \sin[(N-1)\Delta] + \beta_k \cos[(N-1)\Delta] \end{bmatrix}, \tag{14}$$

where $\alpha_k = \sin\theta_k \sin\phi_k$, $\beta_k = \sin\theta_k \cos\phi_k$, and $\Delta = 2\pi/N$.

The received data collected by the CCCP array at time t can be represented as

$$\mathbf{X}(t) = \mathbf{A}\mathbf{S}(t) + \mathbf{N}(t), \tag{15}$$

where $\mathbf{X}(t)$, $\mathbf{S}(t)$, $\mathbf{N}(t)$, and $\mathbf{A}$ are the $2N+2$ received data, the K uncorrelated incident signals, the zero-mean additive complex Gaussian noise, and the steering vector matrix of K incident signals, respectively.

The lower and upper circle subarray steering vectors $\mathbf{A}_1$ and $\mathbf{A}_2$ are constructed by the first $N+1$ rows and the last

$N+1$ rows of vector $\mathbf{A}$. Their relationship can be expressed as

$$\mathbf{A}_2 = \mathbf{A}_1\mathbf{\Phi}, \tag{16}$$

where

$$\mathbf{\Phi} = \begin{bmatrix} e^{j(2\pi d/\lambda)\cos\theta_1} & & \\ & \ddots & \\ & & e^{j(2\pi d/\lambda)\cos\theta_K} \end{bmatrix}. \tag{17}$$

4. Quaternion-ESPRIT Algorithm

The covariance matrix of received data $\mathbf{X}(t)$ is given by

$$\mathbf{R}_{\mathbf{x}} = E\left[\mathbf{X}\mathbf{X}^H\right] = \mathbf{A}\mathbf{R}_s\mathbf{A}^H + \sigma^2\mathbf{I}, \tag{18}$$

with $E[\cdot]$ symbolizing the statistical mean $(\cdot)^H$ denoting the complex conjugate transpose, σ^2 indicating the white noise power and $\mathbf{R}_s = E[\mathbf{s}(t)\mathbf{s}^H(t)]$ representing the source covariance matrix. Let $\mathbf{E}_s$ be the $(2N+2)\times K$ signal subspace matrix composed of the K eigenvectors corresponding to the K largest eigenvalues of $\mathbf{R}_x$ and let $\mathbf{E}_n$ denote the noise subspace composed of the remaining $2N+2-K$ eigenvectors of $\mathbf{R}_x$. According to the subspace theory, there exists $K\times K$ nonsingular matrix $\mathbf{T}$, and the signal subspace can be expressed explicitly as

$$\mathbf{E}_s = \mathbf{A}\mathbf{T}, \tag{19}$$

$\mathbf{E}_1$ and $\mathbf{E}_2$ are constructed directly using the first $N+1$ rows and the last $N+1$ rows of matrix $\mathbf{E}_s$. According to the definition of signal subspace, the relationship of matrices $\mathbf{E}_1$ and $\mathbf{E}_2$ can be showed explicitly as

$$\mathbf{E}_1 = \mathbf{A}_1\mathbf{T}, \qquad \mathbf{E}_2 = \mathbf{A}_2\mathbf{T} = \mathbf{A}_1\mathbf{\Phi}\mathbf{T}. \tag{20}$$

The following expression can be obtained by crunching matrix operation:

$$\mathbf{E}_1^{\#}\mathbf{E}_2\mathbf{T}^{-1} = \mathbf{T}^{-1}\mathbf{\Phi}, \tag{21}$$

where $\mathbf{E}_1^{\#} = (\mathbf{E}_1^H\mathbf{E}_1)^{-1}\mathbf{E}_1^H$.

Let $\mathbf{\Gamma} = \mathbf{E}_1^{\#}\mathbf{E}_2 = (\mathbf{E}_1^{\mathbf{H}}\mathbf{E}_1)^{-1}\mathbf{E}_1^{\mathbf{H}}\mathbf{E}_2$; then (21) can be rewritten as

$$\mathbf{\Gamma}\mathbf{T}^{-1} = \mathbf{T}^{-1}\mathbf{\Phi}. \tag{22}$$

Equation (22) implies that the estimation of $\mathbf{\Phi}$ is a matrix whose diagonal elements are composed of the K largest eigenvalues of matrix $\mathbf{\Gamma}$ and the full-rank matrix $\mathbf{T}^{-1}$ is composed of the K eigenvectors corresponding to the K largest eigenvalues of matrix $\mathbf{\Gamma}$. The estimations of $\mathbf{A}_1$, $\mathbf{A}_2$, and $\mathbf{A}$ can be obtained:

$$\widehat{\mathbf{A}}_1 = \mathbf{E}_1\mathbf{T}^{-1}, \qquad \widehat{\mathbf{A}}_2 = \mathbf{E}_2\mathbf{T}^{-1}, \qquad \widehat{\mathbf{A}} = \mathbf{E}_s\mathbf{T}^{-1}. \tag{23}$$

4.1. The Estimations of DOA. From the expression of $\widehat{\mathbf{\Phi}}$, the estimation of elevation angle can be given as

$$\widehat{\theta}_k = \cos^{-1}\left[\frac{\lambda}{2\pi d}\arg\left(\widehat{\Phi}_{kk}\right)\right]. \tag{24}$$

The elevation obtained by the cosine function in formula (24) can eliminate quadrant ambiguity; the values of elevation can be taken in range from 0 to π.

The estimation of signal spatial steering vector $\widehat{\mathbf{q}}_D(\theta_k,\phi_k)$ is obtained from $\mathbf{A}_1$:

$$\widehat{\mathbf{q}}_D(\theta_k,\phi_k) = \frac{\mathbf{A}_1(:,k)}{\mathbf{A}_1(:,1)} = \begin{bmatrix} 1 \\ \widehat{\mathbf{q}}_L(\theta_k,\phi_k) \end{bmatrix}. \tag{25}$$

From formulas (14) and (25), the following expression can be gotten as follows:

$$\mathbf{\Omega} = \arg\left[\widehat{\mathbf{q}}_L(\theta_k,\phi_k)\right] = \mathbf{W}\cdot\begin{bmatrix}\widehat{\alpha}_k \\ \widehat{\beta}_k\end{bmatrix}, \tag{26}$$

where

$$\mathbf{W} = \frac{2\pi R}{\lambda}\begin{bmatrix} 0 & 1 \\ \sin\Delta & \cos\Delta \\ \vdots & \vdots \\ \sin[(N-1)\Delta] & \cos[(N-1)\Delta] \end{bmatrix}. \tag{27}$$

According to (26), the following expression can be obtained:

$$\begin{bmatrix}\widehat{\alpha}_k \\ \widehat{\beta}_k\end{bmatrix} = \mathbf{W}^{\#}\mathbf{\Omega}, \tag{28}$$

where $\mathbf{W}^{\#} = (\mathbf{W}^H\mathbf{W})^{-1}\mathbf{W}^H$.

From formulas (24) and (28), the estimates of azimuth are given:

$$\begin{aligned} \widehat{\phi}_k &= \arctan\left(\frac{\widehat{\alpha}_k}{\widehat{\beta}_k}\right), \quad \widehat{\beta}_k \geq 0, \\ \widehat{\phi}_k &= \pi + \arctan\left(\frac{\widehat{\alpha}_k}{\widehat{\beta}_k}\right), \quad \widehat{\beta}_k < 0. \end{aligned} \tag{29}$$

4.2. The Estimations of Polarization. According to formulas (10) and (15), the matrix $\mathbf{A}$ can be expressed as another form:

$$\mathbf{A} = \mathbf{A}_e + \mathbf{A}_h j, \tag{30}$$

where $\mathbf{A}_e$ and $\mathbf{A}_h$ are, respectively, the dipole and loop subarray steering vectors, which can be reconstructed from the real and three imaginary parts of $\mathbf{A}$. From (9), (10), and (15), it can be seen that

$$\mathbf{A}_e = \mathbf{A}_h\mathbf{\Psi}, \tag{31}$$

where

$$\mathbf{\Psi} = \begin{bmatrix} -\tan\gamma_1 e^{j\eta_1} & & \\ & \ddots & \\ & & -\tan\gamma_K e^{j\eta_K} \end{bmatrix} = \mathbf{A}_h^{\#}\mathbf{A}_e, \tag{32}$$

with $\mathbf{A}_h^{\#} = (\mathbf{A}_h^H\mathbf{A}_h)^{-1}\mathbf{A}_h^H$ is pseudoinverse matrix of $\mathbf{A}_h$.

According to (32), the polarization parameters estimation are presented as

$$\gamma_k = \tan^{-1}\left(\left|\mathbf{\Psi}_{kk}\right|\right), \qquad \eta_k = \arg\left(-\mathbf{\Psi}_{kk}\right). \tag{33}$$

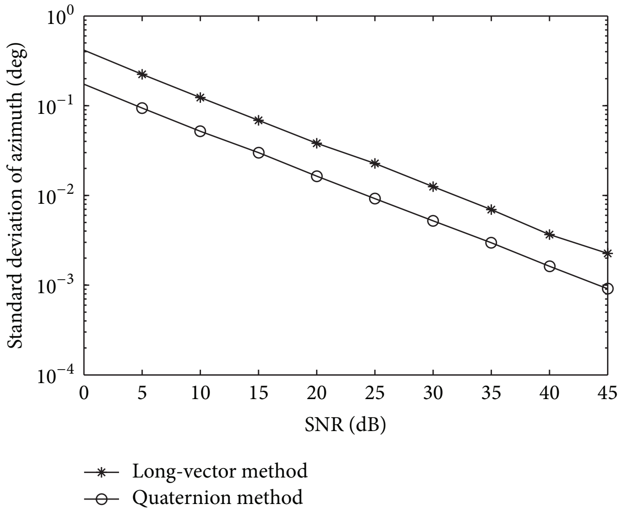

Figure 3: Standard deviation of azimuth versus SNR.

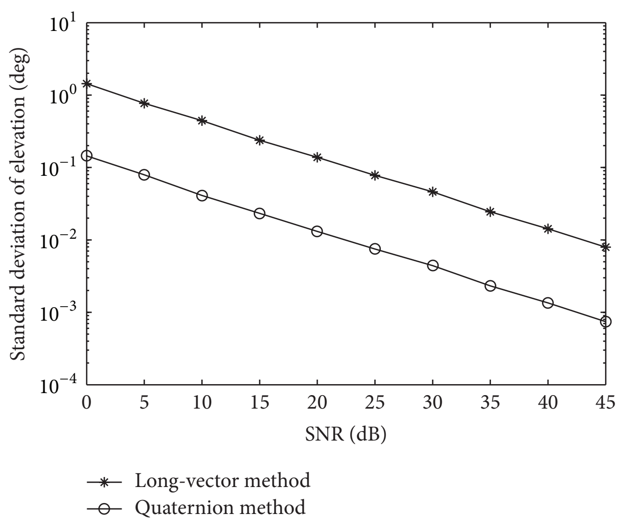

Figure 4: Standard deviation of elevation versus SNR.

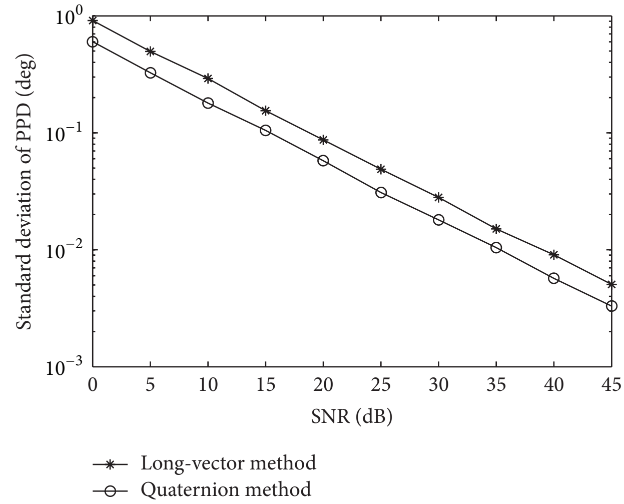

Figure 5: Standard deviation of PPD versus SNR.

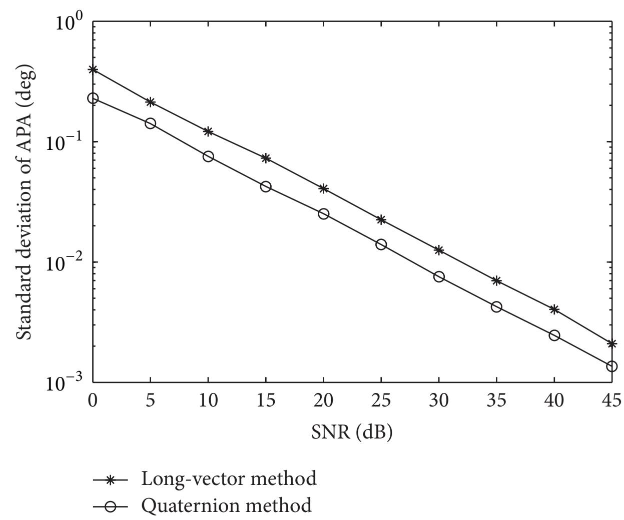

Figure 6: Standard deviation of APA versus SNR.

5. Simulation Results

In this section, some simulations are conducted to evaluate the performances on DOA and polarization estimation by the proposed method. Two uncorrelated equal-powered signals with parameters $(\theta_1, \phi_1, \gamma_1, \eta_1) = (72^\circ, 85^\circ, 30^\circ, 120^\circ)$ and $(\theta_2, \phi_2, \gamma_2, \eta_2) = (30^\circ, 43^\circ, 67^\circ, 80^\circ)$ impinge upon the CCCP array with $N = 6$ CLD pairs sensors. The circle radius of CCCP is $0.5\lambda_{\min}$. The distance of the two circle rings is $0.5\lambda_{\min}$. The signal-to-noise ratio (SNR) is from 0 to 45 dB; 1024 snapshots are used in each of the 500 independent Monte Carlo simulation experiments. The results are shown in Figures 3, 4, 5, and 6.

The solid line with star and circular data points in Figures 3–6 indicates the standard deviations of azimuth, elevation, polarization phase difference (PPD), and auxiliary polarization angle (APA), respectively. The results are estimated by the long-vector and the proposed quaternion methods, at various signal-to-noise ratio (SNR) levels. The proposed quaternion procedure is better than the long vector. The estimation precision at 0 dB based on the quaternion model has improved to be larger than 0.24° for azimuth, 1.29° for elevation, 0.31° for PPD, and 0.17° for APA, compared with that of the long-vector method. Moreover, the standard deviations of azimuth, elevation, PPD, and APA are reduced evidently as the SNR increases using the quaternion method. The enhanced performance is rooted in the special data model of quaternion, which can provide a better signal subspace approximation than the long-vector methods.

6. Conclusion

A quaternion-ESPRIT algorithm for estimating DOA and polarization using CCCP array has been studied in this paper. The novel method can decouple the DOA estimation from the polarization estimation; the DOA and polarization errors herein do not cumulate. The proposed algorithm overcomes quadrant ambiguity in elevation angle when CCCP array is used for wide range elevation angle (more than 90 degrees) estimation. The performance of the proposed method is superior to the long-vector method because the quaternion matrix operations can maintain the vectorial property of the vector sensor and provide a better signal subspace approximation than the long-vector methods.

Conflict of Interests

The authors declare that there is no conflict of interests regarding the publication of this paper.

Acknowledgments

This work was supported by the National Natural Science Foundation of China (61201295, 60971108, and 61101243) and the Fundamental Research Funds for the Central Universities (K5051307017). The authors would like to thank the anonymous reviewers and the associated editor for their valuable comments and suggestions that improved the clarity of this paper.

References

[1] A. Nehorai and E. Paldi, "Vector sensor processing for electromagnetic source localization," in *Proceedings of the 25th Asilomar Conference on Signals, Systems & Computers*, pp. 566–572, Pacific Grove, Calif, USA, November 1991.

[2] A. Nehorai and E. Paldi, "Vector-sensor array processing for electromagnetic source localization," *IEEE Transactions on Signal Processing*, vol. 42, no. 2, pp. 376–398, 1994.

[3] J. Li, "Direction and polarization estimation using arrays with small loops and short dipoles," *IEEE Transactions on Antennas and Propagation*, vol. 41, no. 3, pp. 379–387, 1993.

[4] M. D. Zoltowski and K. T. Wong, "Closed-form eigenstructure-based direction finding using arbitrary but identical subarrays on a sparse uniform Cartesian array grid," *IEEE Transactions on Signal Processing*, vol. 48, no. 8, pp. 2205–2210, 2000.

[5] M. D. Zoltowski and K. T. Wong, "ESPRIT-based 2-D direction finding with a sparse uniform array of electromagnetic vector sensors," *IEEE Transactions on Signal Processing*, vol. 48, no. 8, pp. 2195–2204, 2000.

[6] K. T. Wong and M. D. Zoltowski, "Closed-form direction finding and polarization estimation with arbitrarily spaced electromagnetic vector-sensors at unknown locations," *IEEE Transactions on Antennas and Propagation*, vol. 48, no. 5, pp. 671–681, 2000.

[7] K. T. Wong and M. D. Zoltowski, "Self-Initiating MUSIC-Based direction finding and polarization estimation in spatio-polarizational beamspace," *IEEE Transactions on Antennas and Propagation*, vol. 48, no. 8, pp. 1235–1245, 2000.

[8] K. T. Wong and M. D. Zoltowski, "Uni-vector-sensor ESPRIT for multisource azimuth, elevation, and polarization estimation," *IEEE Transactions on Antennas and Propagation*, vol. 45, no. 10, pp. 1467–1474, 1997.

[9] J. Li, P. Stoica, and D. Zheng, "Efficient direction and polarization estimation with a COLD array," *IEEE Transactions on Antennas and Propagation*, vol. 44, no. 4, pp. 539–547, 1996.

[10] M. N. El Korso, R. Boyer, A. Renaux, and S. Marcos, "Statistical resolution limit of the uniform linear cocentered orthogonal loop and dipole array," *IEEE Transactions on Signal Processing*, vol. 59, no. 1, pp. 425–431, 2011.

[11] X. Yuan, K. T. Wong, and K. Agrawal, "Polarization estimation with a dipole-dipole pair, a Dipole-Loop Pair, or a Loop-Loop Pair of Various Orientations," *IEEE Transactions on Antennas and Propagation*, vol. 60, no. 5, pp. 2442–2452, 2012.

[12] J. Li and R. T. Compton Jr., "Angle and polarization estimation using ESPRIT with a polarization sensitive array," *IEEE Transactions on Antennas and Propagation*, vol. 39, no. 9, pp. 1376–1383, 1991.

[13] J. Li and R. T. Compton Jr., "Two-dimensional angle and polarization estimation using the ESPRIT algorithm," *IEEE Transactions on Antennas and Propagation*, vol. 40, no. 5, pp. 550–555, 1992.

[14] J. Li and R. T. Compton Jr., "Angle estimation using a polarization sensitive array," *IEEE Transactions on Antennas and Propagation*, vol. 39, no. 10, pp. 1539–1543, 1991.

[15] K. T. Wong and A. K.-Y. Lai, "Inexpensive upgrade of base-station dumb antennas by two magnetic loops for "blind" adaptive downlink beamforming," *IEEE Antennas and Propagation Magazine*, vol. 47, no. 1, pp. 189–193, 2005.

[16] K. T. Wong, "Direction finding/polarization estimation-dipole and/or loop triad(s)," *IEEE Transactions on Aerospace and Electronic Systems*, vol. 37, no. 2, pp. 679–684, 2001.

[17] C. K. A. Yeung and K. T. Wong, "CRB: Sinusoid-sources estimation using collocated dipoles/loops," *IEEE Transactions on Aerospace and Electronic Systems*, vol. 45, no. 1, pp. 94–109, 2009.

[18] X. Yuan, "Quad compositions of collocated dipoles and loops: for direction finding and polarization estimation," *IEEE Antennas and Wireless Propagation Letters*, vol. 11, pp. 1044–1047, 2012.

[19] Y. Xu, Z. Liu, K. T. Wong, and J. Cao, "Virtual-manifold ambiguity in HOS-based direction-finding with electromagnetic vector-sensors," *IEEE Transactions on Aerospace and Electronic Systems*, vol. 44, no. 4, pp. 1291–1308, 2008.

[20] Y. Xu, X. Gong, and Z. Liu, "Quad-quaternion MUSIC for DOA estimation using electromagnetic vector sensors," *Eurasip Journal on Advances in Signal Processing*, vol. 2008, Article ID 213293, 2008.

[21] S. Miron, N. Le Bihan, and J. I. Mars, "Quaternion-MUSIC for vector-sensor array processing," *IEEE Transactions on Signal Processing*, vol. 54, no. 4, pp. 1218–1229, 2006.

[22] N. le Bihan, S. Miron, and J. I. Mars, "MUSIC algorithm for vector-sensors array using biquaternions," *IEEE Transactions on Signal Processing*, vol. 55, no. 9, pp. 4523–4533, 2007.

[23] X. Gong, Y. Xu, and Z. Liu, "Quaternion ESPRIT for direction finding with a polarization sentive array," in *Proceedings of the 9th International Conference on Signal Processing (ICSP '08)*, pp. 378–381, Beijing, China, October 2008.

[24] X. Gong, Z. Liu, Y. Xu, and M. Ishtiaq Ahmad, "Direction-of-arrival estimation via twofold mode-projection," *Signal Processing*, vol. 89, no. 5, pp. 831–842, 2009.

[25] X. F. Gong, Z. W. Liu, and Y. G. Xu, "Coherent source localization: Bicomplex polarimetric smoothing with electromagnetic vector-sensors," *IEEE Transactions on Aerospace and Electronic Systems*, vol. 47, no. 3, pp. 2268–2285, 2011.

[26] N. le Bihan and J. Mars, "Singular value decomposition of quaternion matrices: a new tool for vector-sensor signal processing," *Signal Processing*, vol. 84, no. 7, pp. 1177–1199, 2004.

[27] J. Ward, *Quaternions and Cayley Numbers: Algebra and Applications*, Kluwer Academic Publishers, New York, NY, USA, 1997.

[28] L. Josefsson and P. Persson, *Conformal Array Antenna Theory and Design*, IEEE Press Series on Electromagnetic Wave Theory, Wiley, New York, NY, USA, 2006.

[29] C. A. Balanis, *Antenna Theory: Analysis and Design*, Wiley, New York, NY, USA, 2005.

[30] R. C. Hansen, P. T. Bargeliotes, J. Boersma et al., *Conformal Antenna Array Design Handbook*, Department of the Navy, Air Systems Command, 1981.